

Research Article: New Research | Sensory and Motor Systems

Time varying encoding of grasping type and force in the primate motor cortex

<https://doi.org/10.1523/ENEURO.0010-25.2025>

Received: 7 January 2025

Revised: 7 April 2025

Accepted: 11 April 2025

Copyright © 2025 Moreno et al.

This is an open-access article distributed under the terms of the [Creative Commons Attribution 4.0 International license](#), which permits unrestricted use, distribution and reproduction in any medium provided that the original work is properly attributed.

This Early Release article has been peer reviewed and accepted, but has not been through the composition and copyediting processes. The final version may differ slightly in style or formatting and will contain links to any extended data.

Alerts: Sign up at www.eneuro.org/alerts to receive customized email alerts when the fully formatted version of this article is published.

1 **Time varying encoding of grasping type and force in the primate motor**
2 **cortex**

3
4
5 Abbreviated title: Encoding grasping type and force in the motor cortex.

6
7 Adriana Moreno¹, Victor de Lafuente^{1*} & Hugo Merchant^{1*}

8
9 ¹Instituto de Neurobiología, UNAM, Campus Juriquilla. Boulevard Juriquilla No. 3001
10 Querétaro, Qro. 76230 México.

11
12 ***Corresponding authors:** Hugo Merchant (hugomerchant@unam.mx) and Victor de
13 Lafuente (lafuente@unam.mx).

14
15 Number of pages: 22

16 Number of figures: 7

17 Number of words for abstract: 166

18 Number of words for introduction: 791

19 Number of words for discussion: 1897

20
21 **Acknowledgements:** This work was supported by Consejo Nacional de Humanidades,
22 Ciencia y Tecnología (CONAHCYT) Grant: A1-S-8430, UNAM-DGAPA: IG200424, and
23 UNAM-DGAPA-PASPA to H. Merchant, and by CONAHCYT: 319212, UNAM-DGAPA:
24 IN207325 to V. de Lafuente. Adriana Moreno is a doctoral student from Programa de
25 Doctorado en Ciencias Biomédicas, Universidad Nacional Autónoma de México (UNAM)
26 and has received CONAHCYT fellowship 1003309. We thank Luis Prado, Raúl Paulín,
27 María Antonieta Carbajo, and Juan Ortiz for their technical assistance.

28
29 The authors declare no competing financial interests.

30
31
32
33
34
35
36
37

38 **Abstract**

39 The primary motor cortex (M1) is strongly engaged by movement planning and execution.
40 However, the role of M1 activity in voluntary grasping is still not completely understood. Here
41 we analyze recordings of M1 neurons during the execution of a delayed reach-to-grasp task,
42 where monkeys had to actively grasp an object with either a side or a precision grip, and
43 then pull it with a low or high amount of force. Single cell and neural populations analyses
44 showed that grip type was robustly and specifically encoded by a large population of
45 neurons, while force level was weakly and transiently encoded within mixed-selective
46 neurons that also encoded grip type. Notably, the grip type was stably decoded from motor
47 cortical populations during the preparation and execution epochs of the task. Our results are
48 consistent with the idea that planning and performing specific grasping movements are high-
49 level skills that strongly engage M1 neurons, while the execution of pulling force might be
50 prominently encoded at lower stages of the motor system.

51

52 **Significance statement**

53 Grasping behavior requires precise motor coordination exerted by multiple brain areas,
54 including the primary motor cortex (M1), but the exact role of M1 in grasping preparation
55 and execution remains elusive. Here, we analyzed the neural activity of M1 while two
56 monkeys performed a delayed reach-to-grasp task. We found that two parameters of
57 grasping: grip type and pulling-force level were encoded in the activity of single neurons and
58 the neural population, although with important differences. While grip coding was stronger
59 and more temporally stable, force encoding was weaker and short lived. Our results suggest
60 that grip planning and execution is a high-level neural process that takes place
61 independently of force control in M1.

62 Introduction

63 Primates, including humans, often manipulate objects using their sophisticated prehensile
64 hands. After determining an object's position in space, we must estimate object features like
65 size, shape, texture, and weight. This information is then used by the brain to plan and
66 execute precise movements to hold it appropriately. These movements comprise two main
67 phases: a reaching phase in which the hand approaches the object, and a grasping phase
68 that occurs once contact is made. During the reaching phase, as the hand moves, the
69 position of the fingers changes, adapting to features of the object we intend to grasp
70 (*reshaping*). During the grasping phase, the position of the hand keeps adapting as the
71 brain receives feedback from tactile and proprioceptive inputs (Jeannerod et al., 1995).
72 Human and monkey hands are capable of different types of grips, including a highly
73 controlled precision grip, in which an object is held between the palmar aspects of the fingers
74 and the opposing thumb (Almécija & Sherwood, 2016). Besides controlling hand position
75 and its derivatives, it is also crucial to regulate the amount of grasping force. If we apply too
76 little force, the object may slip out of our hands, whereas if we apply too much, it may break
77 or become damaged. Throughout the years, efforts have been made to determine how the
78 brain gives rise to this highly precise and controlled behavior.

79 Due to M1's spinal projections, which include direct monosynaptic connections to
80 spinal motoneurons, earlier studies aimed to find correlations between M1 neural activity
81 and muscle activation (Strick et al., 2021). Surprisingly, the responses of M1 neurons
82 showed to be highly diverse. While the firing rates of some neurons do correlate with muscle
83 activation during single-joint movements and isometric force control (Cheney & Fetz, 1980;
84 Evarts, 1968; Maier et al., 1993; T. M. J. Wannier et al., 1991), others seem to carry
85 information about parametric aspects of reaching kinematics like direction, speed, trajectory
86 and dynamic force changes (Georgopoulos et al., 1986, 1992, 2007; Hatsopoulos et al.,
87 2007; Inoue et al., 2018; Merchant et al., 2004; Naselaris et al., 2006a, 2006b). In addition,
88 recent studies have revealed that M1 neural populations can be described as a dynamical
89 system in which internally generated temporal patterns generate motor commands that are
90 sent to the spinal motoneurons and eventually, effector muscles (Churchland et al., 2012;
91 Russo et al., 2018). In addition, it has been shown that M1 activity correlates with movement
92 preparation, with population responses that converge to a particular state space when the
93 system has encoded all the properties of the upcoming reaching movement (Afshar et al.,
94 2011; Churchland et al., 2006; Riehle & Requin, 1993).

95 The motor cortex is also part of a cortical network that controls the visuomotor
96 transformations for goal related grasping movements. This network includes, in hierarchical
97 order: the anterior intraparietal area, areas 7a and 7ab of the posterior parietal cortex, ventral
98 premotor cortex (F5p), and M1. Neurons in this network encode the visual features of the
99 objects to be grasped, as well as the movement parameters associated with the type of grip
100 needed for grasping (Brochier & Umiltà, 2007). Indeed, M1 neurons are not only tuned to
101 different types of grips (Lemon et al. 1986; Mason et al. 2002) but also to the force exerted
102 to grasp an object (Intveld et al., 2018). Nevertheless, grasping type recruits motor cortical
103 activity to a larger degree as compared to grasping force, with a mostly independent control
104 of the two parameters (Hendrix et al., 2009; Rastogi et al., 2021). In addition, M1 is also
105 involved in the preparatory phase of grasping commands, where the population dynamics

106 adopt different state trajectories during the preparation for different types of grasping
107 movements (Meirhaeghe et al., 2023).

108 Here, we performed encoding and decoding analyses on the activity of
109 simultaneously recorded M1 neurons from two monkeys performing a delayed reach-to-
110 grasp task (Brochier et al., 2018). As shown before, we corroborate that at the single-unit
111 and population levels, grip type had a profound effect on motor cortical activity, while force
112 level explained less variance of the neural responses. We found that this was achieved
113 through a combination of more neurons representing grip, as well as enhanced grip coding
114 at the single-unit level. Notably, our analyses show that several neurons were modulated
115 only by grip type, while force was encoded by neurons selective for both grip and force.
116 Furthermore, the neural signals linked to grip type emerged right after grip instruction and
117 were maintained after movement onset, forming a long-lasting and stable preparatory signal
118 for precision or side grip that extended through movement execution. Importantly, even while
119 pulling the object, when force level and grip type are simultaneously executed, force level
120 transiently engaged fewer neurons and accounted for a small proportion of activity variance.

121

122 **Materials and methods**

123 *Behavioral task*

124 We analyzed the online database generously made public by Brochier et. al (2018), who
125 designed and performed all the experiments shown here. The task and recording methods
126 are explained in detail elsewhere (Brochier et al., 2018). Briefly, two macaque monkeys
127 (*macaca mulatta*): N (male) and L (female), were trained in a delayed reach-to-grasp task,
128 in which they were visually instructed to grasp an object using either a side grip or a precision
129 grip. After grasping, the monkeys had to pull the object for at least 500 ms with either a low
130 or a high force level. From now on, we will refer to the amount of force required to pull the
131 object as 'force'. Monkeys were rewarded with a drop of apple sauce at the end of the trial
132 if they followed the grip and force instructions correctly. Figure 1 shows the sequence of
133 events that defined each trial of the reach-to-grasp task. Note that grip type and force level
134 cues were temporally separated. The monkeys were first instructed about grip type, and
135 after a 1 s delay, they were given an additional visual cue to indicate force magnitude. The
136 force level cue also served as the go-cue to initiate the hand movement. Thus, monkeys
137 had an established time window of 1 s (delay period) for grip preparation, while no explicit
138 epoch was designated for force preparation, forcing the animals to prepare force level 'on
139 the go', as the arm was moving. This also meant that, while grip preparation could be
140 temporally isolated, grip execution as well as force planning and execution overlapped
141 during the movement period of the task. Reaction time (RT) was defined as the time elapsed
142 between the go-cue and the start of the reaching movement. Movement time (MT) was
143 calculated as the time from movement onset until the object was touched.

144 *Neural recordings*

145 Neural recordings were collected and preprocessed by Brochier et al. (2018). Briefly, a 10-
146 by-10 Utah electrode array (Blackrock Microsystems, Salt Lake City, UT, USA) was
147 chronically implanted in the primary motor (M1) and premotor cortex (dorsally in monkey L
148 and more ventrally in monkey N) on the right hemisphere of each monkey, contralateral to

149 the working hand. Neural signals from a total of 96 electrodes were amplified, high pass
150 filtered (0.3 Hz – 7.5 kHz) and digitized with a sampling rate of 30 kHz. Raw signals were
151 online high-pass filtered at 250 Hz and spike waveforms were detected by threshold
152 crossing (manually set). To isolate single-unit activity, both online and offline sorting were
153 performed. Manual online sorting was performed first for inspection, using Central Suite
154 (Blackrock Microsystems, Salt Lake City, UT, USA). For all the analyses shown here, we
155 considered only isolated units resulting from the offline sorting performed by the data
156 providers (Brochier et al., 2018). Offline sorting was performed using Plexon Offline Sorter
157 (Plexon Inc, Dallas, Texas, USA). Cross-threshold unsorted waveforms were split into
158 clusters in a 2- or 3-dimensional principal component space. K-Means and Valley Seeking
159 algorithms were used to sort waveforms coming from different units. Further inspection using
160 inter-spike (ISI) distributions and auto-correlation and cross-correlation plots was performed
161 to differentiate single-unit from multi-unit activity. Since we focused only on motor cortical
162 activity, we considered neural signals coming only from electrodes located posterior to the
163 putative border between M1 and the premotor cortex (61 sites for monkey N and 68 sites
164 for monkey L). In total, we analyzed neural data coming from 110 isolated units in the case
165 of monkey N and 97 units for monkey L. We analyzed a total of two sessions (one session
166 per animal) consisting of 137 trials for monkey N, and 135 trials for monkey L. We considered
167 only correct trials for all the analyses shown.

168 *Single-unit analysis*

169 To study activity at single-unit level, we calculated the firing rate of each neuron as a function
170 of time by using a causal exponential filter with a decay rate of 100 ms displaced every 20
171 ms. For each neuron, firing rates were averaged across trials and aligned to the onset of the
172 reaching movement.

173 To characterize firing rate modulations of individual neurons in response to grip and
174 force conditions, we calculated the area under the curve of the receiver operating
175 characteristic (auROC) as a function of time. The auROC estimates the overlap between
176 two distributions. For each neuron, the distributions compared are the firing rates of one
177 condition versus its counterpart condition (side grip trials vs precision grip trials; and high
178 force trials vs low force trials). An auROC value of 0.5 indicates that distributions completely
179 overlapped and thus, firing rates are not useful to differentiate the two conditions. We
180 calculated each neuron's auROC as a function of time and then performed a non-parametric
181 permutation test to identify time points at which auROC was different from 0.5 ($p < 0.001$).
182 In addition, if a neuron had a significant auROC for at least two consecutive time bins
183 (permutation test for multiple comparisons, $p < 0.001$), then it was considered to significantly
184 encode the tested parameter (de Lafuente & Romo, 2006; Merchant et al., 1997).

185 To determine whether single cell grip and force encoding were independent from
186 each other, we first measured whether their modulation directionality was dependent on
187 each other. For this, we performed a X^2 test that compared the expected versus the
188 observed marginal distributions of the grip and force auROC values for all cells and for each
189 time bin (Figure 4, middle panels) throughout the entire time series of the task. The expected
190 marginal is the product of the observed probability of grip type (Figure 4A-D, right scatter
191 yellow distribution on the right) by the observed probability of pulling force (Figure 4A-D,
192 right scatter purple top distribution), while the observed marginal corresponds to the
193 probability of observing both parameters in the actual data (computing the 2D histograms of

194 the combined distributions (yellow and purple). In addition, we computed the 2D normal
195 distribution on this data, obtaining ellipses whose angle can reveal dependency between
196 parameters, where an angle close to 90 degrees would indicate independence.

197 Next, we performed a correlation analysis to determine whether the modulation
198 strengths of both parameters covaried. For this, we first estimated the ΔauROC , which is the
199 absolute value of the difference between each neuron's auROC and 0.5. We then performed
200 a non-parametric correlation test, in which we shuffled ΔauROC data across both time and
201 neurons (1000 times, without replacement). We obtained the Pearson correlation coefficient
202 of each shuffle (between shuffled 'force' ΔauROC s and shuffled 'grip' ΔauROC values at
203 each time point). We considered these null distributions and then estimated the true Pearson
204 correlation coefficient between grip ΔauROC s and force ΔauROC s as a function of time and
205 considered it significant when $p < 0.001$ for at least two consecutive time bins (permutation
206 test for multiple comparisons, $p < 0.001$).

207 In addition to these tests, we also performed a cross-temporal correlation analysis,
208 in which we compared grip ΔauROC s at each time point vs lagged force ΔauROC values
209 (ranging from -400 ms to 400 ms, relative to the tested grip bin). The obtained Pearson
210 correlation coefficients were tested against a shuffled (null) distribution (1000 repetitions, no
211 replacement, $p < 0.001$), for each time bin and lag. Correlations were considered significant
212 if at least two consecutive time bins were significantly correlated (permutation test for
213 multiple comparisons, $p < 0.001$).

214 *Neural population analysis*

215 To determine whether the neural population of M1 encodes grip type and force level, we
216 performed a demixed principal component analysis (Kobak et al., 2016). Similarly to
217 principal component analysis (PCA), dPCA is a dimensionality-reduction method that allows
218 to extract the neural population components that explain most variance (Gómez et al.,
219 2019a). In dPCA these components are referred to as 'demixed' because they explain
220 variance attributed to specific task variables. In our case, the demixed principal components
221 (dPCs) were associated with grip type, force level, and temporal events within the task
222 (referred to as condition-independent activity). Additionally, to detect the time points at which
223 task parameters were significantly encoded by the neural population at the single-trial level,
224 three linear classifiers were constructed using the first dPCs (i.e., that explained most
225 variance) associated to each variable of interest (grip, force and interaction) to decode task
226 conditions. For each classifier, a stratified Monte Carlo leave-group-out cross-validation was
227 performed. Monte Carlo chance distribution was set to 100 and time periods when the actual
228 classification accuracy exceeded shuffled decoding accuracies in at least 10 consecutive
229 time bins, were considered significant.

230 *Neural population decoding*

231 A decoding analysis was implemented using a methodology developed by Crowe et al.,
232 (Crowe et al., 2014), and Merchant and Averbeck (Merchant & Averbeck, 2017). For each
233 neuron, the discharge rate was computed in 100 ms time bins within -2000 to 2000 ms
234 relative to movement onset, resulting in 51 time-bins, across the 30 trials of the two grip and
235 two force conditions. For each time bin, we built an SVM classifier with a 10-fold cross-
236 validation. The procedure was repeated 50 times using different training ($n = 25$) and testing
237 ($n = 5$) trials each time, and the prediction results were averaged between repetitions.

238 Accuracy thus estimated classifier's ability to discriminate the experimental conditions and
239 corresponds to the total correctly predicted trials divided by the total number trials for each
240 tested condition (2 for grip type or 2 for pulling force). A 50% accuracy corresponds to a
241 random classification performance for the two levels of each parameter.

242 We carried out a cross-temporal decoding analysis in which we trained and tested
243 the SVMs using all possible combinations of 100-ms time bins to establish the temporal
244 evolution of grip and force coding (Mohan et al., 2021; Pearl et al., 2024). This analysis
245 results in a classification accuracy matrix where the values along the diagonal are calculated
246 by performing training and testing on equivalent time bins (Figures 6B, 7B). In contrast,
247 different time bins are used for training and testing and calculating the off-diagonal accuracy
248 values. The off-diagonal accuracy allows us to determine how stable in time is a neural
249 population signal when compared with the on-diagonal values. In fact, we considered an off-
250 diagonal accuracy bin-pair combination as static, namely, a bin combination that shows
251 decoding generalization from the on-diagonal bin classification model, when the three
252 following conditions were met. The off-diagonal accuracy was significantly higher than
253 chance (cluster-based permutation test, $p < 0.01$), was above the 99% of the bootstrapped
254 null distribution (1000 iterations with shuffled classification labels), and that the two
255 corresponding time bins on-diagonal showed a classification accuracy above chance level
256 (permutation test, $p < 0.01$, Bonferroni corrected for the number of on-diagonal time bins).
257 Next, we computed a binary matrix of the same size as the cross-temporal decoding matrix,
258 where we assigned 1 to at least two consecutive time bins resulting as static and 0 for all
259 remaining time bins. Then, we quantified the magnitude of cross-time decoding between
260 and within the two main task epochs using the generalization index. The generalization index
261 provides information about the proportion of SVM tested bins during the preparation and
262 execution that were classified as static during the trained bins of either the preparation or
263 execution epoch.

264 *Code accessibility*

265 The dataset analyzed in this paper was collected, described and made public by Brochier et
266 al. (Brochier et al., 2018), and can be freely accessed using the following link:
267 <https://doi.gin.g-node.org/10.12751/g-node.f83565/>. The custom MATLAB code used to
268 perform the analyses shown here is also freely available
269 (<https://github.com/MerchantLabINB/GraspForce2025>).

270

271 **Results**

272 *Monkeys were able to use two grip types and two force levels to grasp and pull an object*

273 In the delayed reach-to-grasp task monkeys were instructed to grasp a cubic object using
274 either a side or a precision grip. Once grasped, the monkeys had to pull and hold the object
275 for at least 500 ms with a low or high amount of force. Figure 1A shows the main events of
276 the task. Each trial started with the monkey placing its left hand over a table switch. After
277 800 ms, a visual cue was displayed for 300 ms, instructing the monkey about grip type. After
278 a 1000 ms delay, an additional visual cue indicated the required force level to pull the object.
279 This cue also served as a go cue for the monkey to start the reaching movement. Thus, this
280 task was designed to determine the neural underpinnings of movement preparation and

281 execution of multijoint complex hand movements, and the neural signals related with the
282 execution of two types of grasping movements combined with two levels of pulling force.

283 The behavioral results show that monkey L performed the task faster, with shorter
284 and less variable reaction times (Figure 1B; mean \pm SD: 150 ms \pm 48 ms) compared to
285 monkey N (mean \pm SD: 251 ms \pm 190 ms). Movement times were also shorter and less
286 variable in monkey L as compared to monkey N (Figure 1C; mean \pm SD; monkey L: 123 ms
287 \pm 80 ms, monkey N: 343 ms \pm 125 ms). Both parameters were significantly different between
288 animals (reaction time: $z = -11.51$, $p = 1.07 \times 10^{-30}$; movement time: $z = -14.01$, $p = 1.29 \times 10^{-44}$,
289 Mann Whitney U-test).

290 *Grip type has a larger influence in M1 neurons compared to force level*

291 We analyzed a total of 110 units for monkey N and 97 units for monkey L. Figure 2A shows
292 the raster plot and firing rate of a neuron from monkey N that increased its activity after
293 movement onset, with a preference for side over precision grip trials. Note that, as the
294 monkey's hand approached the object (object touch), activity started to become modulated
295 also by force level. Figure 2B shows a neuron that fired strongly during precision grip trials.
296 Figure 2C illustrates a neuron that fired more during the preparation and execution of a side
297 grip and a low force level. Finally, Figure 2D depicts a neuron that is more active during
298 preparation and execution of a precision grip and a high force level.

299 To determine whether single-unit activity contained information about task
300 parameters, we computed the area under the curve of the receiver operating characteristic
301 (auROC), comparing side vs precision grip trials (grip), and low vs high force trials (force)
302 (see Methods). Neural activity was aligned to movement onset. The heatmaps in Figure 3A-
303 B show the absolute value of the difference between auROC values and 0.5 (Δ auROC), for
304 neurons with significant firing rate modulations for either grip type (left panel) or force level
305 (right panel; permutation test, $p < 0.001$). Neurons were sorted by the time of their maximum
306 Δ auROC value. In monkey N, the average Δ auROC peaked after movement onset for most
307 neurons, while maximum force Δ auROC occurred later, after object touch. It is worth noting
308 that grip- and force-encoding peaks span large temporal windows, and this can be
309 interpreted as a dynamic activation chain in which neurons successively encode movement
310 parameters, with especially brief selective periods for force level. This type of population
311 dynamics has been reported in numerous cortical areas during different behavioral tasks
312 (Crowe et al., 2014; Gámez et al., 2019; Mendoza et al., 2018, 2024; Merchant et al., 2015).
313 In addition, the time profile of Δ auROC clearly indicates that individual neurons were less
314 modulated by force as compared to grip (Figure 3C-D). Note also that monkey L reached
315 higher Δ auROC values for both parameters and exhibited a stronger preparatory signal for
316 grip type, compared to monkey N.

317 Next, we identified and grouped neurons according to the modulations in their firing
318 rates by both parameters. In monkey N, we found 57 neurons that were significantly
319 modulated by grip type, while 21 were tuned to both grip and force. We found similar
320 proportions in monkey L, with 47 units being modulated only by grip, while 33 were mixed-
321 selective for both parameters. In both animals, only a small number of neurons ($n = 2$, for
322 each monkey) were significantly modulated by force only, indicating that most of the force
323 encoding in M1 occurs through neurons that are also modulated by grip. Figure 4A (right)
324 shows the average Δ auROC for grip and force as a function of time, across neurons that

325 were modulated only by grip type, in monkey N (left). The middle panel shows each neuron's
326 grip auROC values as a function of force auROCs, 400 ms after movement onset for the
327 same subpopulation. Notice how the rotation angle of the 95%-confidence interval (blue
328 ellipse) is close to 90°. This indicates that, while the firing of most of these neurons is
329 modulated by grip type (auROC values uniformly distributed along the y-axis), the
330 directionality of these modulations does not covary with force's (i.e. neurons that have
331 preference for one grip do not necessarily have preference towards a specific force level).
332 To formally test this, we performed an independence test, comparing the two marginal
333 distributions of grip and force auROCs throughout the entire time series (see Methods). We
334 did not find a significant dependence between the directionality of grip and force encoding
335 at any time bin (permuted X^2 test, $p < 0.001$). The same analysis was performed using units
336 that encoded both grip and force and we found similar results (Figure 4B). The absence of
337 dependence between grip and force encoding was also observed in monkey L (Figure 4,
338 middle panels C and D).

339 It is possible that, even when the directionality of firing rate modulations is
340 independent between parameters, a correlation between the strength of these modulations
341 exists. Therefore, we performed a correlation analysis between grip and force modulations,
342 now comparing the absolute changes in auROC (Δ auROC) instead of their raw values. We
343 did not find significant correlations between the strength of grip and force-related
344 modulations at any time point in any of the neural subpopulations analyzed (permutation
345 test, $p < 0.001$). Figure 4 (right panels) shows grip Δ auROC as a function of force Δ auROC
346 values for each neuron during a time point close to the mean time when each monkey
347 touched the object (400 ms for monkey N and 160 ms for monkey L). Lastly, we performed
348 the same correlation analysis 'cross-temporally', comparing grip vs lagged force Δ auROC
349 values (ranging from -400 ms to 400 ms). We found sparse and brief correlations (for 3 bins
350 or less) in the mixed-selective subpopulations of both monkeys (data not shown).

351 These findings suggest that grip and force might be encoded as separate entities in
352 motor cortical cells, even when individual units are modulated by both parameters. Although,
353 this effect may be partially affected by temporal differences between both signals, given that
354 force encoding emerges later in the task.

355 *Population encoding of grip type and force level*

356 We performed a population analysis using demixed principal components (dPCs) which
357 estimated the percentage of variance associated with (1) condition-independent
358 modulations (related to the temporal structure of the task), (2) grip type, and (3) force level
359 Figure 5A shows the normalized firing rates of all M1 neurons projected onto dPC #1 for
360 monkeys N (left) and L (right). We found that the largest proportion of population variance is
361 explained by condition-independent activity that is related to the temporal structure of the
362 task, i.e. to the moment at which the monkeys initiate and release the grasp on the object.

363 It is interesting to note that dPC #1 in monkey N showed a less pronounced slope in
364 the increase of activity associated with movement onset, and this might be related to the
365 slower reaction and movement times of the animal compared to monkey L. This increase
366 was maintained during the entire movement period, with activity decreasing after object
367 release. Conversely, neural temporal dynamics on monkey L were overall faster, with a more

368 pronounced slope during the peri-movement period and a sudden drop after object touch.
369 This was followed by a small increase in activity in response to object release.

370 The dynamics of the dPCs related to grip type are shown in Figure 5B. It must be
371 noted that the amount of variance associated with grip type in both animals is an order of
372 magnitude smaller compared to that related to the temporal structure of the task. In the case
373 of monkey N, dPC #8 explained 1.9% of total variance, but this was enough to decode hand
374 grip at the single-trial level, before movement onset. For monkey L, dPC #5 explained 3.5%
375 of total variance and allowed to predict the monkey's hand grip hundreds of milliseconds
376 before the animal received the go cue. Grip encoding was maintained until the monkey
377 released the object and was not held any further, as opposed to what we observed in
378 monkey N.

379 The dynamics of the activity related to force level are shown in Figure 5C. In monkey
380 N, dPC #17 explained 0.2% of total variance, and it allowed to decode force level later in the
381 trials and for shorter time windows, compared to grip type. For monkey L, dPC #12 allowed
382 to predict force trials more consistently, from movement onset until hundreds of milliseconds
383 before object release. Figure 5D and 5E show the total explained variance for each task
384 variable in monkey N and monkey L, respectively. In both cases, condition-independent
385 components explained about 90% of total neural variance. This was followed by grip that
386 explained 6% and 7% of total variance in monkey N and L, respectively. Force explained
387 only 2% of variance in the case of monkey N and 1% for monkey L. The interaction of grip
388 and force explained less than 2% of total variance and interestingly, none of its associated
389 dPCs allowed above-chance decoding of task condition at the single-trial level, hence they
390 were not considered to be significant.

391 *Relation between behavior and neural decoding*

392 To assess whether the neural population encoding captured by the main dPCs correlated
393 with the actual pulling force, we measured the correlation between the exerted pulling force
394 as a function of time and condition-independent and force-related dPCs from M1 neurons.
395 First, it is evident that both monkeys performed the task properly, applying force only after
396 the go signal and with no force changes during the delay period (Figure 5-1A). As expected,
397 the exerted force level was higher during the high force trials. However, as evidenced by the
398 dPCA analysis, the time profiles of force and time decoding varied between monkeys. While
399 monkey N exhibited more tonic neural modulations that resembled the sustained application
400 of force, neural decoding of time and force was more phasic, differing from the tonic pulling-
401 force signal. This comes in agreement with previous studies describing diverse time profiles
402 of force-related neural responses that do not necessarily equal force application time
403 (Cheney & Fetz, 1980; Hendrix et al., 2009; Wannier et al., 1991). Furthermore, the
404 correlations between the applied force and the force dPCs were smaller than those between
405 the applied force and the condition-independent (time) dPCs for both animals (Figure 5-1,
406 panels D and E).

407 *Population activity allows decoding grip type and force level during single trials*

408 Given that the neurons were simultaneously recorded, we used SVM classifiers to test
409 whether population activity allowed the decoding of grip type and force during single trials.
410 Figures 6A and 7A show the decoding accuracy of the grip type and grip-force classifiers as
411 a function of time in monkeys N and L, respectively. For both animals, the above-chance

412 decoding for grip type started almost immediately after the onset of the grip cue and
413 continued during movement execution. In contrast, significant decoding of force level was
414 present only during movement execution and its magnitude was smaller than for grip. Next,
415 to assess how stable grip and force encoding were throughout time, we performed a cross-
416 temporal decoding analysis. Specifically, we trained and tested both classifiers using all
417 possible pairs of time bins during the peri-movement period of the task. This method
418 produces a classification accuracy matrix where the off-diagonal values are a measure of
419 how generalizable the neural encoding of grip type or force at a particular time bin is, when
420 directly compared with the corresponding diagonal values, where the training (x-axis) and
421 testing (y-axis) of the classifier are over the same time bin. Hence, the level of generalization
422 across time bins tells us how consistently a set of neurons encode grip type or force across
423 time during task performance. Figures 6B and 7B show the heatmaps of the cross-temporal
424 decoding accuracies for grip and force classifiers using neural activity from monkeys N and
425 L, respectively. For monkey L, grip decoding was more stable in time (static), with two
426 generalization clusters, one during movement preparation, and another during grip
427 execution. This is more evident in the binary matrix of Figure 7D, where the significant static
428 off-decoding bins are depicted in yellow.

429 In contrast to grip type, force decoding was temporally less stable (dynamic), with
430 only a few significant off-diagonal time bins, all of them close to the on-diagonal time bins,
431 and that occurred only during the movement execution (Figure 7D). In the case of monkey
432 N, grip type decoding was also more temporally stable than force (Figure 6B). However,
433 stable time bins were distributed more sparsely across preparation and execution periods,
434 with more static bins clustered within the execution period of the task.

435 We developed a generalization index that corresponds to the proportion of SVM bins
436 that were classified as static when cross-temporally decoding grip and force across the
437 preparation and execution epochs of the task. Hence, these indexes summarize how the
438 significant decoding during the preparation epoch generalizes within the preparation and for
439 the execution, or how the significant decoding during execution generalizes for the
440 preparation and execution epochs. Figures 6C and 7C show the generalization index as a
441 function of test time when the classifier was trained during preparation (blue line) and
442 execution (red) for monkeys N and L, respectively. It is evident that there is a generalization
443 of grip type decoding from preparation to execution and vice versa, suggesting that the motor
444 cortical populations possessed information about the type of grip across task epochs,
445 although there is a clear bias for a larger number of static bins when training and testing the
446 classifier in the same epoch. Interestingly, grip type generalization was more pronounced
447 during preparation for monkey N, whereas decoding during execution generalized more in
448 monkey L.

449 **Discussion**

450 In this study we aimed to explore the role of primate's cortical area M1 during a reach-to-
451 grasp behavioral task that required the precise regulation of two parameters: grip type and
452 force level. Our findings support three conclusions. First, we found that at the single-unit and
453 population levels, grip type had a larger effect on motor cortical activity, while the force level
454 was weak and transiently encoded by single units and explained less neural variance.
455 Second, grip type was encoded through movement preparation and execution, while force
456 encoding was brief and emerged later during movement execution. Importantly, grip type

457 was encoded by both grip-selective and mixed-selective cells, while force was encoded
458 mostly by mixed-selective cells. Analyzing the marginal probabilities in the selectivity of cells
459 we found no interaction between the two parameters, supporting the notion that grip type
460 and pulling force are coded as separate entities in the motor cortex. The lack of significant
461 interaction between grip type and pulling force in the demixed PCA corroborated this finding
462 at the neural population level. Third, the neural modulations linked to grip type emerged right
463 after grip instruction and were maintained after movement onset, forming a long lasting and
464 stable signal for precision or side grip during the preparation and execution epochs of the
465 task. Thus, the categorical grip signal was more static compared to force, which occurred
466 later and was more phasic. Our findings support the notion that M1 is strongly engaged in
467 encoding grip type, with neural populations distinguishing between the two grips across the
468 preparation and execution epochs of the task. In contrast, force was encoded transiently
469 during movement execution and was mostly independent of grip type.

470 *Grip type is encoded at both single-unit and population levels in M1*

471 For both animals, most neurons were strongly modulated by grip. Neural coding of grip
472 emerged during the delay period and peaked near movement onset. Since monkeys had to
473 perform either a side or a precision grip, it is important to highlight the differences between
474 them, especially in the motor coordination required for each. While a side grip demands the
475 coordination of the thumb and the rest of the fingers as a group, a precision grip is a finer,
476 and therefore a more controlled movement, that requires independent coordination of the
477 fingers to grasp an object using only the thumb and the index finger (Almécija & Sherwood,
478 2016; Edin et al., 1992; Jeannerod et al., 1995). A previous study has shown that M1
479 neurons fire more during a precision grip compared to a power grip (Muir & Lemon, 1983).
480 This neural modulation does not seem to represent muscle engagement exclusively, since
481 there is not an absolute correlation between net force and the firing rate of individual neurons
482 of the pyramidal tract in M1 (Maier et al., 1993; Muir & Lemon, 1983). A possibility is that
483 action complexity and therefore, the level of motor control needed, could modulate neural
484 activity, and send specific motor commands to the spinal cord related to different hand grips
485 (Muir & Lemon, 1983). Whether neural activity in M1 represents muscles or movements has
486 been a topic of debate for years. Evidence supports the notion that both can be equally
487 represented in M1 neural activity (Takei et al., 1999; Wang et al., 2022). Our results show
488 that grip type was encoded at the neural population level and dPCA analysis of population
489 activity demonstrated that, in both animals, grip encoding emerges during the delay period,
490 while the animals prepare the movement. Similar to what we found at the single-unit level,
491 significant decoding of grip was possible earlier in monkey L, almost immediately after the
492 grip cue. In addition, our findings at the neural population-level are consistent with what has
493 been previously reported in the literature for M1 and other grasping-related areas like the
494 anterior intraparietal area (AIP) and the anterior portion of the ventral premotor cortex (area
495 F5), in which time is the most represented task parameter, followed by grip and lastly, force
496 (Intveld et al., 2018; Rastogi et al., 2021).

497 *Force level is weakly encoded at both single-unit and population levels in M1*

498 We found that force level elicited weaker modulations in the firing rate of individual neurons
499 compared to grip type. Moreover, we found fewer force-coding neurons, compared to grip-
500 coding neurons. Interestingly, most of these cells were co-modulated by grip, which
501 implicates that the coding of force in M1 occurs through mixed-selective neural

502 subpopulations mostly (Kobak et al., 2016; Rigotti et al., 2013). At the population level we
503 found that force also explained less neural variance than grip, consistent with what we found
504 in single units.

505 At first, we considered that a possible explanation for the differences between grip
506 and force coding could reside on the time the animals had to prepare both. We thought of
507 the possibility that having less time to prepare the appropriate force level could impact on
508 the amount of explained variance within the neural population of M1. However, other studies
509 using an extended version of this dataset found that, even when the monkeys are instructed
510 first on the load force level (reverse condition), classification accuracy of force using local-
511 field potentials (LFPs) remains lower than grip (Milekovic et al., 2015). Moreover, a previous
512 study using dPCA to characterize the population coding of grip type and grip force in
513 grasping-related areas, including M1, also showed that grip force explained less neural
514 variance than grip type, even when both grip and force were simultaneously planned within
515 the same time window (Intveld et al., 2018). Therefore, our results agree with such previous
516 findings.

517 Remarkably, the force-encoding subpopulations showed brief activation profiles
518 with selectivity for the low-force and others for the high-force conditions, suggesting that
519 force might not be encoded linearly in M1 neural activity. These M1 neural properties
520 contrast with the steady pulling force exerted by the monkeys after movement onset, which
521 was by task design, larger for the high force condition. Therefore, the transient and non-
522 linear encoding of force suggests that M1 might generate categorical signals that are read
523 and transformed downstream to control the actual hand pulling force.

524 *Grip and force might be encoded as independent parameters in M1 at both single-unit and*
525 *population level*

526 Several studies have found that motor-related areas like the posterior parietal cortex (PPC),
527 AIP, the dorsal and ventral premotor cortices (PMd and PMv, respectively) and M1 actively
528 participate in grip and force control during grasping (Chib et al., 2009; Davare et al., 2006;
529 Intveld et al., 2018). However, whether these aspects of grasping behavior are part of the
530 same neural process, or if they are driven by different neural mechanisms, has been a topic
531 of debate (Cheney et al., 1980; Churchland et al., 2012; Evarts, 1968; Georgopoulos et al.,
532 1986; Taira et al., 1996; Tanji & Evarts, 1976). While some studies have pointed to a
533 common neural substrate for grip and force control in M1 (Hepp-Reymond et al., 1999; Maier
534 et al., 1993), more recent findings suggest that these parameters might be represented
535 independently of each other in motor and premotor areas in both single units and the neural
536 population (Hendrix et al., 2009; Intveld et al., 2018). Accordingly, our findings demonstrate
537 that the neurons that were selective for both grip type and pulling force covered the four
538 possible encoding scenarios (side/precision grip, low/high force) with no correlation in both
539 the modulation directionality and strength of the two parameters across motor cortical
540 neurons. Furthermore, a lack of dependence between grip and force encoding could also
541 be seen at the population level, with no significant interaction between grip and force
542 encoding, as evidenced by the dPCA. Taken together, our results support the idea that the
543 motor cortex may maintain the neural signals for grip and force as separate entities mostly.
544 However, to fully corroborate this, further observations regarding this feature should be
545 made in tasks in which grip type and force level planning times are similar.

546 *Grip encoding is more stable than force in M1*

547 Lastly, we evaluated the temporal stability of grip and force encoding. We found that grip
548 coding was stable in time (hence, static) during the preparation and execution epochs of the
549 task. The cross-temporal decoding analysis suggests that similar populations of neurons
550 maintained information about the grip type for hundreds of milliseconds in both epochs of
551 the task. In addition, since the analysis of the applied force revealed that monkeys only
552 exerted grasping force after the go cue, this analysis supports the notion that grasping-
553 selective responses during the delay period are linked to movement preparation. The neural
554 mechanisms behind the static coding scheme are still being studied. However, it has been
555 proposed that neural representations are sustained in time by reverberating connections
556 between pyramidal neurons (Merchant et al., 2003; Romo et al., 1996) through activation of
557 NMDA receptors (Wang et al., 2013). To further explore the static coding of grip in M1, we
558 developed a generalization index as a measure of the temporal generalization of grip
559 encoding across preparatory and executive periods of the task by the same neural
560 population (Crowe et al., 2010; Crowe et al., 2014; Gámez et al., 2019). We found that grip
561 encoding generalizes across both periods of the task despite the temporal differences in
562 movement timing between animals. Therefore, our results indicate that M1 neural
563 populations can keep a sustained coding of grip type during preparation and execution of
564 movement. We did not observe this during force coding, which was more dynamic. We
565 expected dynamic force coding, since the cueing of the pulling force magnitude did not allow
566 for explicit force preparation. In addition, the lack of temporal generalization in force
567 decoding might be related to the limited modulation strength in M1 by the pulling force
568 magnitude. Taken together, these results suggest that the encoding of task-relevant
569 movement parameters in M1 can be embedded in distinct coding schemes that change
570 flexibly, according to task demands. A previous study has shown that static and dynamic
571 coding schemes can coexist within the same cortical area (i.e. the prefrontal cortex) and it
572 is possible to switch from one to another according to the task requirements and learning
573 (Ceccarelli et al., 2023).

574 In summary, we found that grip type and force level are encoded as independent
575 parameters in M1 neural activity during grasping at both single-unit and population levels.
576 Coding of grip type was carried by both mixed-selective and grip-selective neurons, while
577 force was encoded by mixed-selective neurons mostly. These neural modulations do not
578 seem to be associated with stereotyped muscle activation patterns of each movement. In
579 both animals, grip type was more strongly encoded than force and such coding scheme was
580 static, engaging similar neural populations across task epochs. On the other hand, force
581 encoding was short lived. This indicates that M1, like some associative areas such as the
582 prefrontal cortex (Ceccarelli et al., 2023; Merchant et al., 2011) can switch from a static to a
583 dynamic coding scheme in response to task demands. Furthermore, we consider it important
584 to remark that for this study, we used a public database, generously shared to the scientific
585 community by the laboratory of Dr. Alexa Riehle. This promotes data analyses that employ
586 a variety of metrics and advances our knowledge of the neural bases of grasping behavior
587 in non-human primates. This practice is becoming more popular and will enormously
588 potentiate systems neuroscience (Hartig et al., 2023; Messinger et al., 2021; Milham et al.,
589 2020).

590 **References**

- 591 Afshar, A., Santhanam, G., Yu, B. M., Ryu, S. I., Sahani, M., & Shenoy, K. V. (2011). Single-
592 Trial Neural Correlates of Arm Movement Preparation. *Neuron*, 71(3), 555–564.
593 <https://doi.org/10.1016/j.neuron.2011.05.047>
- 594 Almécija, S., & Sherwood, C. C. (2016). Hands, Brains, and Precision Grips: Origins of Tool
595 Use Behaviors. In *Evolution of Nervous Systems: Second Edition* (Vols. 3–4, pp. 299–
596 315). Elsevier Inc. <https://doi.org/10.1016/B978-0-12-804042-3.00085-3>
- 597 Brochier, T., & Umiltà, M. A. (2007). Cortical control of grasp in non-human primates. *Current*
598 *Opinion in Neurobiology*, 17(6), 637–643. <https://doi.org/10.1016/j.conb.2007.12.002>
- 599 Brochier, T., Zehl, L., Hao, Y., Duret, M., Sprenger, J., Denker, M., Grün, S., & Riehle, A.
600 (2018). Massively parallel recordings in macaque motor cortex during an instructed
601 delayed reach-to-grasp task. *Scientific Data*, 5(1), 180055.
602 <https://doi.org/10.1038/sdata.2018.55>
- 603 Ceccarelli, F., Ferrucci, L., Londei, F., Ramawat, S., Brunamonti, E., & Genovesio, A. (2023).
604 Static and dynamic coding in distinct cell types during associative learning in the
605 prefrontal cortex. *Nature Communications*, 14(1), 8325.
606 <https://doi.org/10.1038/s41467-023-43712-2>
- 607 Cheney, P. D., & Fetz, E. E. (1980). Functional classes of primate corticomotoneuronal cells
608 and their relation to active force. *Journal of Neurophysiology*, 44(4), 773–791.
609 <https://doi.org/10.1152/jn.1980.44.4.773>
- 610 Chib, V. S., Krutky, M. A., Lynch, K. M., & Mussa-Ivaldi, F. A. (2009). The Separate Neural
611 Control of Hand Movements and Contact Forces. *The Journal of Neuroscience*, 29(12),
612 3939–3947. <https://doi.org/10.1523/JNEUROSCI.5856-08.2009>
- 613 Churchland, M. M., Cunningham, J. P., Kaufman, M. T., Foster, J. D., Nuyujukian, P., Ryu,
614 S. I., & Shenoy, K. V. (2012). Neural population dynamics during reaching. *Nature*,
615 487(7405), 51–56. <https://doi.org/10.1038/nature11129>
- 616 Churchland, M. M., Yu, B. M., Ryu, S. I., Santhanam, G., & Shenoy, K. V. (2006). Neural
617 Variability in Premotor Cortex Provides a Signature of Motor Preparation. *The Journal*
618 *of Neuroscience*, 26(14), 3697–3712. <https://doi.org/10.1523/JNEUROSCI.3762-05.2006>
- 620 Crowe, D. A., Zarco, W., Bartolo, R., & Merchant, H. (2014). Dynamic representation of the
621 temporal and sequential structure of rhythmic movements in the primate medial
622 premotor cortex. *Journal of Neuroscience*, 34(36), 11972–11983.
623 <https://doi.org/10.1523/JNEUROSCI.2177-14.2014>
- 624 Davare, M., Andres, M., Cosnard, G., Thonnard, J.-L., & Olivier, E. (2006). Dissociating the
625 Role of Ventral and Dorsal Premotor Cortex in Precision Grasping. *The Journal of*
626 *Neuroscience*, 26(8), 2260–2268. <https://doi.org/10.1523/JNEUROSCI.3386-05.2006>
- 627 de Lafuente, V., & Romo, R. (2006). Neural correlate of subjective sensory experience
628 gradually builds up across cortical areas. *Proceedings of the National Academy of*
629 *Sciences*, 103(39), 14266–14271. <https://doi.org/10.1073/pnas.0605826103>

- 630 Edin, B. B., Westling, G., & Johansson, R. S. (1992). Independent control of human finger-
631 tip forces at individual digits during precision lifting. *The Journal of Physiology*, 450(1),
632 547–564. <https://doi.org/10.1113/jphysiol.1992.sp019142>
- 633 Evarts, E. V. (1968). Relation of pyramidal tract activity to force exerted during voluntary
634 movement. *Journal of Neurophysiology*, 31(1), 14–27.
635 <https://doi.org/10.1152/jn.1968.31.1.14>
- 636 Gámez, J., Mendoza, G., Prado, L., Betancourt, A., & Merchant, H. (2019). The amplitude
637 in periodic neural state trajectories underlies the tempo of rhythmic tapping. *PLOS*
638 *Biology*, 17(4), e3000054. <https://doi.org/10.1371/journal.pbio.3000054>
- 639 Georgopoulos, A. P., Ashe, J., Smyrnis, N., & Taira, M. (1992). The Motor Cortex and the
640 Coding of Force. *Science*, 256(5064), 1692–1695.
641 <https://doi.org/10.1126/science.256.5064.1692>
- 642 Georgopoulos, A. P., Merchant, H., Naselaris, T., & Amirkian, B. (2007). Mapping of the
643 preferred direction in the motor cortex. *Proceedings of the National Academy of*
644 *Sciences*, 104(26), 11068–11072. <https://doi.org/10.1073/pnas.0611597104>
- 645 Georgopoulos, A., Schwartz, A., & Kettner, R. (1986). Neuronal Population Coding of
646 Movement Direction. *Science*, 233(4771), 1416–1419.
647 <https://doi.org/10.1126/science.3749885>
- 648 Hartig, R., Klink, P. C., Polyakova, Z., Dehaqani, M. R. A., Bondar, I., Merchant, H.,
649 Vanduffel, W., Roe, A. W., Nambu, A., Thirumala, M., Shmuel, A., Kapoor, V., Gothard,
650 K. M., Evrard, H. C., Basso, M. A., Petkov, C. I., & Mitchell, A. S. (2023). A framework
651 and resource for global collaboration in non-human primate neuroscience. In *Current*
652 *Research in Neurobiology* (Vol. 4). Elsevier B.V.
653 <https://doi.org/10.1016/j.crneur.2023.100079>
- 654 Hatsopoulos, N. G., Xu, Q., & Amit, Y. (2007). Encoding of Movement Fragments in the
655 Motor Cortex. *The Journal of Neuroscience*, 27(19), 5105–5114.
656 <https://doi.org/10.1523/JNEUROSCI.3570-06.2007>
- 657 Hendrix, C. M., Mason, C. R., & Ebner, T. J. (2009). Signaling of Grasp Dimension and
658 Grasp Force in Dorsal Premotor Cortex and Primary Motor Cortex Neurons During
659 Reach to Grasp in the Monkey. *Journal of Neurophysiology*, 102(1), 132–145.
660 <https://doi.org/10.1152/jn.00016.2009>
- 661 Hepp-Reymond, M.-C., Kirkpatrick-Tanner, M., Gabernet, L., Qi, H.-X., & Weber, B. (1999).
662 Context-dependent force coding in motor and premotor cortical areas. *Experimental*
663 *Brain Research*, 128(1–2), 123–133. <https://doi.org/10.1007/s002210050827>
- 664 Inoue, Y., Mao, H., Suway, S. B., Orellana, J., & Schwartz, A. B. (2018). Decoding arm
665 speed during reaching. *Nature Communications*, 9(1), 5243.
666 <https://doi.org/10.1038/s41467-018-07647-3>
- 667 Intveld, R. W., Dann, B., Michaels, J. A., & Scherberger, H. (2018). Neural coding of intended
668 and executed grasp force in macaque areas AIP, F5, and M1. *Scientific Reports*, 8(1),
669 17985. <https://doi.org/10.1038/s41598-018-35488-z>

- 670 Jeannerod, M., Arbib, M. A., Rizzolatti, G., & Sakata, H. (1995). Grasping objects: the
671 cortical mechanisms of visuomotor transformation. *Trends in Neurosciences*, 18(7),
672 314–320. [https://doi.org/10.1016/0166-2236\(95\)93921-J](https://doi.org/10.1016/0166-2236(95)93921-J)
- 673 Kakei, S., Hoffman, D. S., & Strick, P. L. (1999). Muscle and Movement Representations in
674 the Primary Motor Cortex. *Science*, 285(5436), 2136–2139.
675 <https://doi.org/10.1126/science.285.5436.2136>
- 676 Kobak, D., Brendel, W., Constantinidis, C., Feierstein, C. E., Kepecs, A., Mainen, Z. F., Qi,
677 X.-L., Romo, R., Uchida, N., & Machens, C. K. (2016). Demixed principal component
678 analysis of neural population data. *ELife*. <https://doi.org/10.7554/eLife.10989.001>
- 679 Lemon, R. N., Mantel, G. W., Muir, R. B., (1986). Corticospinal facilitation of hand muscles
680 during voluntary movement in the conscious monkey. *The Journal of*
681 *Physiology*, 381 doi: 10.1113/jphysiol.1986.sp016341
- 682 Maier, M. A., Bennett, K. M., Hepp-Reymond, M. C., & Lemon, R. N. (1993). Contribution of
683 the monkey corticomotoneuronal system to the control of force in precision grip. *Journal*
684 *of Neurophysiology*, 69(3), 772–785. <https://doi.org/10.1152/jn.1993.69.3.772>
- 685 Mason C. R., Gomez J. E., Ebner T. J. (2002). Primary motor cortex neuronal discharge
686 during reach-to-grasp: controlling the hand as a unit. *Archives Italiennes de Biologie*.
687 140(3), 229-236. PMID: 12173526.
- 688 Meirhaeghe, N., Riehle, A., & Brochier, T. (2023). Parallel movement planning is achieved
689 via an optimal preparatory state in motor cortex. *Cell Reports*, 42(2), 112136.
690 <https://doi.org/10.1016/j.celrep.2023.112136>
- 691 Mendoza, G., Fonseca, E., Merchant, H., & Gutierrez, R. (2024). Neuronal Sequences and
692 dynamic coding of water-sucrose categorization in rat gustatory cortices. *IScience*,
693 27(12), 111287. <https://doi.org/10.1016/j.isci.2024.111287>
- 694 Mendoza, G., Méndez, J. C., Pérez, O., Prado, L., & Merchant, H. (2018). Neural basis for
695 categorical boundaries in the primate pre-SMA during relative categorization of time
696 intervals. *Nature Communications*, 9(1). <https://doi.org/10.1038/s41467-018-03482-8>
- 697 Merchant, H., & Averbeck, B. B. (2017). The Computational and Neural Basis of Rhythmic
698 Timing in Medial Premotor Cortex. *The Journal of Neuroscience*, 37(17), 4552–4564.
699 <https://doi.org/10.1523/JNEUROSCI.0367-17.2017>
- 700 Merchant, H., Battaglia-Mayer, A., & Georgopoulos, A. P. (2003). Functional organization of
701 parietal neuronal responses to optic-flow stimuli. *Journal of Neurophysiology*, 90(2),
702 675–682. <https://doi.org/10.1152/jn.00331.2003>
- 703 Merchant, H., Battaglia-Mayer, A., & Georgopoulos, A. P. (2004). Neural Responses during
704 Interception of Real and Apparent Circularly Moving Stimuli in Motor Cortex and Area
705 7a. *Cerebral Cortex*, 14(3), 314–331. <https://doi.org/10.1093/cercor/bhg130>
- 706 Merchant, H., Crowe, D. A., Robertson, M. S., Fortes, A. F., & Georgopoulos, A. P. (2011).
707 Top-Down Spatial Categorization Signal from Prefrontal to Posterior Parietal Cortex in
708 the Primate. *Frontiers in Systems Neuroscience*, 5.
709 <https://doi.org/10.3389/fnsys.2011.00069>

- 710 Merchant, H., Pérez, O., Bartolo, R., Méndez, J. C., Mendoza, G., Gámez, J., Yc, K., &
711 Prado, L. (2015). Sensorimotor neural dynamics during isochronous tapping in the
712 medial premotor cortex of the macaque. *European Journal of Neuroscience*, 41(5),
713 586–602. <https://doi.org/10.1111/ejn.12811>
- 714 Merchant, H., Zainos, A., Hernández, A., Salinas, E., & Romo, R. (1997). Functional
715 Properties of Primate Putamen Neurons During the Categorization of Tactile Stimuli.
716 *Journal of Neurophysiology*, 77(3), 1132–1154.
717 <https://doi.org/10.1152/jn.1997.77.3.1132>
- 718 Messinger, A., Sirmipilatze, N., Heuer, K., Loh, K. K., Mars, R. B., Sein, J., Xu, T., Glen, D.,
719 Jung, B., Seidlitz, J., Taylor, P., Toro, R., Garza-Villarreal, E. A., Sponheim, C., Wang,
720 X., Benn, R. A., Cagna, B., Dadarwal, R., Evrard, H. C., ... Klink, P. C. (2021). A
721 collaborative resource platform for non-human primate neuroimaging. *NeuroImage*,
722 226. <https://doi.org/10.1016/j.neuroimage.2020.117519>
- 723 Milekovic, T., Truccolo, W., Grün, S., Riehle, A., & Brochier, T. (2015). Local field potentials
724 in primate motor cortex encode grasp kinetic parameters. *NeuroImage*, 114, 338–355.
725 <https://doi.org/10.1016/j.neuroimage.2015.04.008>
- 726 Milham, M., Petkov, C. I., Margulies, D. S., Schroeder, C. E., Basso, M. A., Belin, P., Fair,
727 D. A., Fox, A., Kastner, S., Mars, R. B., Messinger, A., Poirier, C., Vanduffel, W., Van
728 Essen, D. C., Alvand, A., Becker, Y., Ben Hamed, S., Benn, A., Bodin, C., ... Zhou, Y.
729 di. (2020). Accelerating the Evolution of Nonhuman Primate Neuroimaging. *Neuron*,
730 105(4), 600–603. <https://doi.org/10.1016/j.neuron.2019.12.023>
- 731 Mohan, K., Zhu, O., & Freedman, D. J. (2021). Interaction between neuronal encoding and
732 population dynamics during categorization task switching in parietal cortex. *Neuron*,
733 109(4), 700-712.e4. <https://doi.org/10.1016/j.neuron.2020.11.022>
- 734 Muir, R. B., & Lemon, R. N. (1983). Corticospinal neurons with a special role in precision
735 grip. *Brain Research*, 261(2), 312–316. [https://doi.org/10.1016/0006-8993\(83\)90635-2](https://doi.org/10.1016/0006-8993(83)90635-2)
- 736 Naselaris, T., Merchant, H., Amirikian, B., & Georgopoulos, A. P. (2006a). Large-scale
737 organization of preferred directions in the motor cortex. I. Motor cortical hyperacuity for
738 forward reaching. *Journal of Neurophysiology*, 96(6), 3231–3236.
739 <https://doi.org/10.1152/jn.00487.2006>
- 740 Naselaris, T., Merchant, H., Amirikian, B., & Georgopoulos, A. P. (2006b). Large-scale
741 organization of preferred directions in the motor cortex. II. Analysis of local distributions.
742 *Journal of Neurophysiology*, 96(6), 3237–3247.
743 <https://doi.org/10.1152/jn.00488.2006> Pearl, J. E., Matsumoto, N., Hayashi, K.,
744 Matsuda, K., Miura, K., Nagai, Y., Miyakawa, N., Minamimoto, T., Saunders, R. C.,
745 Sugase-Miyamoto, Y., Richmond, B. J., & Eldridge, M. A. G. (2024). Neural Correlates
746 of Category Learning in Monkey Inferior Temporal Cortex. *Journal of Neuroscience*,
747 44(49). <https://doi.org/10.1523/JNEUROSCI.0312-24.2024>
- 748 Rastogi, A., Willett, F. R., Abreu, J., Crowder, D. C., Murphy, B. A., Memberg, W. D., Vargas-
749 Irwin, C. E., Miller, J. P., Sweet, J., Walter, B. L., Rezaii, P. G., Stavisky, S. D.,
750 Hochberg, L. R., Shenoy, K. V., Henderson, J. M., Kirsch, R. F., & Ajiboye, A. B. (2021).

751 The neural representation of force across grasp types in motor cortex of humans with
752 tetraplegia. *ENeuro*, 8(1), 1–23. <https://doi.org/10.1523/ENEURO.0231-20.2020>

753 Riehle, A., & Requin, J. (1993). The predictive value for performance speed of preparatory
754 changes in neuronal activity of the monkey motor and premotor cortex. *Behavioural*
755 *Brain Research*, 53(1–2), 35–49. [https://doi.org/10.1016/S0166-4328\(05\)80264-5](https://doi.org/10.1016/S0166-4328(05)80264-5)

756 Rigotti, M., Barak, O., Warden, M. R., Wang, X.-J., Daw, N. D., Miller, E. K., & Fusi, S.
757 (2013). The importance of mixed selectivity in complex cognitive tasks. *Nature*,
758 497(7451), 585–590. <https://doi.org/10.1038/nature12160>

759 Romo, R., Merchant, H., Zainos, A., & Hernández, A. (1996). Categorization of somaesthetic
760 stimuli: sensorimotor performance and neuronal activity in primary somatic sensory
761 cortex of awake monkeys. *Neuroreport*, 7(7), 1273–1279.
762 <http://www.ncbi.nlm.nih.gov/pubmed/8817548>

763 Russo, A. A., Bittner, S. R., Perkins, S. M., Seely, J. S., London, B. M., Lara, A. H., Miri, A.,
764 Marshall, N. J., Kohn, A., Jessell, T. M., Abbott, L. F., Cunningham, J. P., & Churchland,
765 M. M. (2018). Motor Cortex Embeds Muscle-like Commands in an Untangled
766 Population Response. *Neuron*, 97(4), 953-966.e8.
767 <https://doi.org/10.1016/j.neuron.2018.01.004>

768 Strick, P. L., Dum, R. P., Rathelot, J.-A., (2021). The Cortical Motor Areas and the
769 Emergence of Motor Skills: A Neuroanatomical Perspective. *Annual Review of*
770 *Neuroscience*, 44(1), 425-447. <https://doi.org/10.1146/annurev-neuro-070918-050216>.

771 Taira, M., Boline, J., Smyrnis, N., Georgopoulos, A. P., & Ashe, J. (1996). On the relations
772 between single cell activity in the motor cortex and the direction and magnitude of three-
773 dimensional static isometric force. *Experimental Brain Research*, 109(3), 367–376.
774 <https://doi.org/10.1007/BF00229620>

775 Tanji, J., & Evarts, E. V. (1976). Anticipatory activity of motor cortex neurons in relation to
776 direction of an intended movement. *Journal of Neurophysiology*, 39(5), 1062–1068.
777 <https://doi.org/10.1152/jn.1976.39.5.1062>

778 Wang, M., Yang, Y., Wang, C.-J., Gamo, N. J., Jin, L. E., Mazer, J. A., Morrison, J. H., Wang,
779 X.-J., & Arnsten, A. F. T. (2013). NMDA Receptors Subserve Persistent Neuronal Firing
780 during Working Memory in Dorsolateral Prefrontal Cortex. *Neuron*, 77(4), 736–749.
781 <https://doi.org/10.1016/j.neuron.2012.12.032>

782 Wang, T., Chen, Y., & Cui, H. (2022). From Parametric Representation to Dynamical
783 System: Shifting Views of the Motor Cortex in Motor Control. *Neuroscience Bulletin*,
784 38(7), 796–808. <https://doi.org/10.1007/s12264-022-00832-x>

785 Wannier, T. M., Maier, M. A., & Hepp-Reymond, M. C. (1991). Contrasting properties of
786 monkey somatosensory and motor cortex neurons activated during the control of force
787 in precision grip. *Journal of Neurophysiology*, 65(3), 572–589.
788 <https://doi.org/10.1152/jn.1991.65.3.572>

789

790 **Figure legends**

791 **Figure 1. Delayed reach-to-grasp task.** A: Monkeys are instructed to grasp and pull an
792 object using a specific hand grip and force level. Each trial starts with the monkey placing
793 its working hand over a table switch (Switch on). After 800 ms, a visual cue indicates the
794 type of grip (precision grip or side grip). After a 1000 ms delay, another visual cue (Go)
795 instructs the monkey to start the reach movement, as well as the amount of force (low or
796 high) needed to pull the object. Reaction time (RT) was measured as the time between the
797 Go cue and the movement onset (Movement on). Movement time (MT) was defined as the
798 time between the movement onset and the object touch (Touch). Once grasped, the monkey
799 must pull the object (Pull On) for at least 500 ms with the instructed force level. If the monkey
800 performs correctly, it is rewarded with a drop of apple sauce (Reward). B: Reaction times
801 during correct trials for monkey N and monkey L, respectively. C: Movement times for both
802 monkeys, displayed as in B.

803 **Figure 2. Four example neurons of M1 during the delayed reach-to-grasp task.** A-B
804 (top): Raster plot of two example neurons from monkey N. Trials are grouped according to
805 the instructed grip type and force level, as indicated by the legends on the left (from bottom
806 to top: side grip and low force, side grip and high force, precision grip and low force, precision
807 grip and high force). Activity is aligned to movement onset (grey solid line). Colored markers
808 indicate task events around movement onset: Go cue (dark red), object touch (red), pull
809 onset (lilac). A-B (bottom): Trial-averaged firing rate across task conditions. Line color
810 indicates grip type (red for side grip and yellow for precision grip). Line style indicates force
811 level (dashed line for high force and solid line for low force). Blue shading indicates the mean
812 reaction time and green shading indicates mean movement time. C-D: Activity of two
813 example neurons from monkey L (same conventions as in A and B).

814 **Figure 3. M1 single units are modulated by grip type and force level.** A: Heatmaps of
815 grip (left) and force (right) coding in single units, using the area under the curve of the
816 Receiver-Operating-Characteristic (auROC) for monkey N. Only neurons with significant
817 tuning for each parameter are shown (auROC significantly away from 0.5; permutation test,
818 $p < 0.001$). B: Same as in A, for monkey L. C: Average grip (left) and force (right) Δ auROC
819 across neurons as a function of time for monkey N. Grey shading indicates the duration of
820 the grip cue. Blue and green shadings indicate mean reaction and movement times,
821 respectively. Black solid line indicates movement onset. The grey dashed line indicates the
822 mean object release time. D: Same as in C, for monkey L.

823 **Figure 4. Grip and force neural modulations are not correlated.** A (left): Average
824 Δ auROC related to grip (yellow solid line) and force (purple solid line) as a function of time
825 for neurons that showed significant tuning for grip type only (only grip), in monkey N
826 (permutation test, $p < 0.001$, $n = 57$ neurons). A (middle): grip as a function of force auROC
827 values, for only-grip coding neurons, 400 ms after movement onset (object touch). Each
828 blue dot represents a neuron. Blue ellipse represents the 95%-confidence interval of the 2-
829 D distribution. θ is the angle of rotation of the ellipse. Purple and yellow histograms at top x
830 and right y axes are the distributions of the auROC values for force and grip, respectively.
831 A (right): grip as a function of force Δ auROCs for only-grip selective neurons, 400 ms after
832 movement onset. Red solid line is the simple linear regression model fitted to the data. The
833 correlation coefficient (R) and the p-value (p) are indicated at the top right. B: Same as in A,
834 for neurons that coded both grip and force significantly (permutation test, $p < 0.001$, $n = 21$

835 neurons) in monkey N. C: same as in A, for monkey L (160 ms after movement onset, only-
836 grip neurons, $n = 47$. Permutation test, $p < 0.001$). D: same as in B, for monkey L (160 ms
837 after movement onset, grip-and-force neurons, $n = 33$. Permutation test, $p < 0.001$).

838 **Figure 5. Population-level coding of grip type and force level in M1 using dPCA.** Firing
839 rates were projected onto the demixed principal component (dPC) that explains the most
840 variance associated with each task parameter (condition-independent, grip and force). A:
841 First condition-independent component (component #1) for monkey N (left) and monkey L
842 (right). B: First significant grip component for monkey N (component #8, left) and monkey L
843 (component #5, right). C: First significant component associated with force for monkey N
844 (component #17, left) and monkey L (component #12, right). Activity was aligned to
845 movement onset (vertical black solid line). Grey shading indicates the duration of the grip
846 cue. Blue and green shadings indicate mean reaction and movement times respectively.
847 Vertical dashed line corresponds to the average time of object release. Component number
848 and percentage of explained variance are shown at the top right corner of each panel. Black
849 solid line at the bottom indicates time points at which the task parameter could be decoded
850 from the neural activity at single-trial level using its associated dPC as a classifier. D:
851 Percentages of total explained variance by each task parameter for monkey N. E: Same as
852 in D, for monkey L. Correlations between main dPCs (condition-independent and force-
853 related) and pulling-force signals were measured and are shown in Figure 5-1.

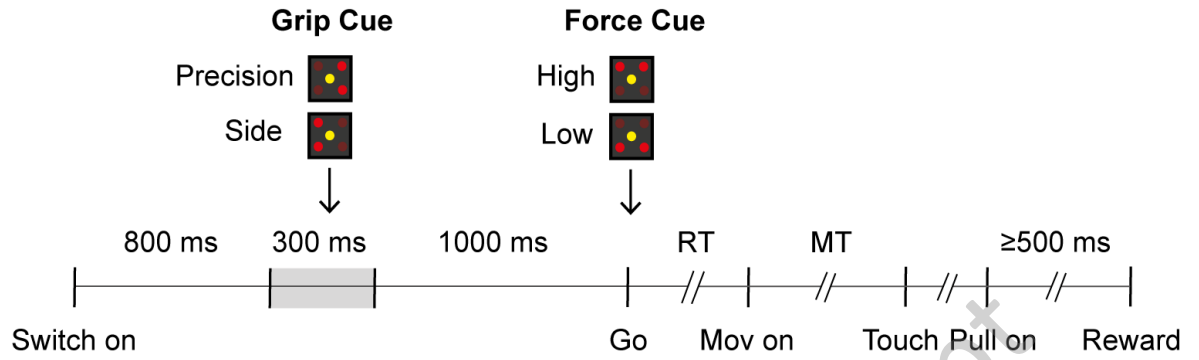
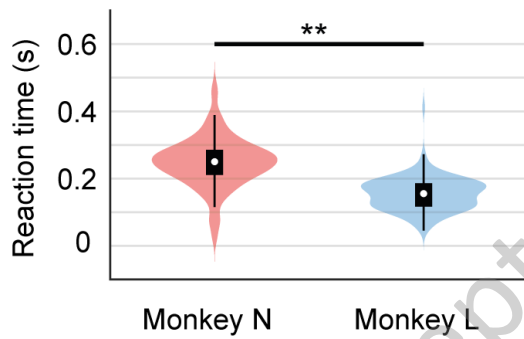
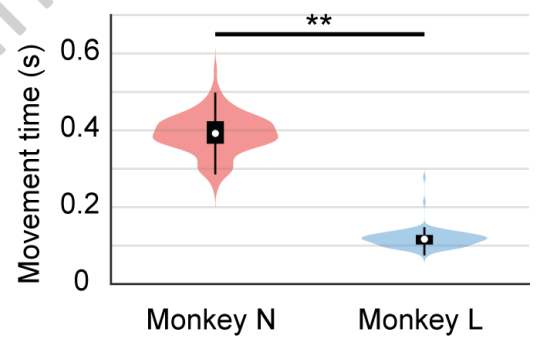
854 **Figure 6. Temporal stability of grip and force encoding in M1 (monkey N).** A: Decoding
855 accuracy of grip type (yellow solid line) and force level (purple solid line) as a function of
856 time using an SVM classifier. Solid lines at the top indicate the times at which accuracy was
857 significantly above chance ($p < 0.01$). Neural activity was aligned to movement onset,
858 indicated by the black vertical line. Gray shading indicates display of the grip cue. Blue and
859 green shadings indicate mean reaction and movement times, respectively. The vertical
860 dashed line corresponds to the average time of object release. B: Cross-temporal decoding
861 of grip (left) and force (right) during the peri-movement period of the task. C: Generalization
862 index, estimated as the proportion of static bins resulting from the cross-temporal decoding
863 of grip as a function of time when training and testing the classifier during preparatory and
864 executive periods of the task. D: Stable time points of the cross-temporal decoding of grip
865 (left) and force (right). Yellow squares indicate significantly stable time bins.

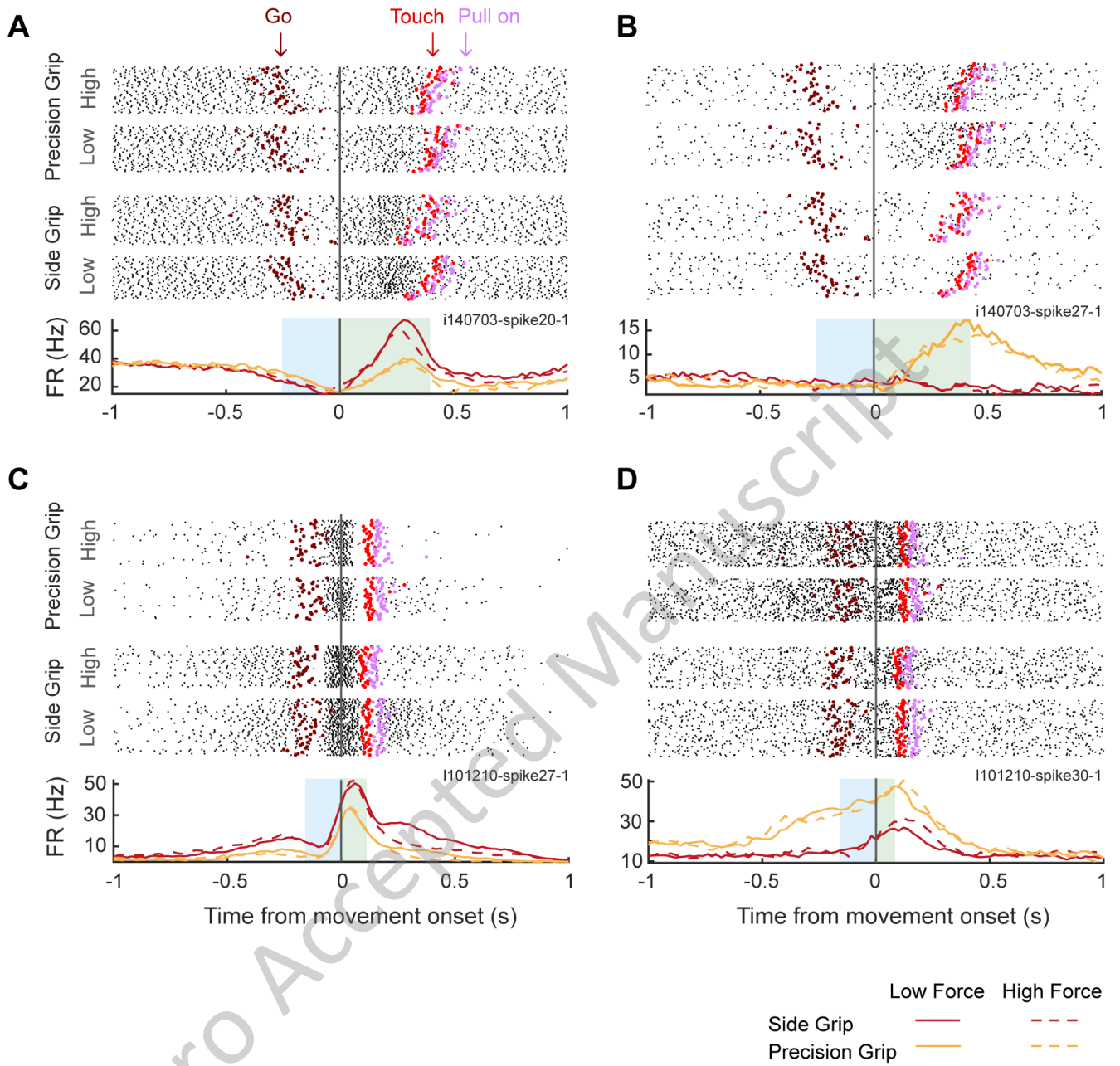
866 **Figure 7. Temporal stability of grip and force encoding in M1 (monkey L).** A: Decoding
867 accuracy of grip type (yellow solid line) and force level (purple solid line) as a function of
868 time using an SVM classifier. Solid lines at the top indicate the times at which accuracy was
869 significantly above chance ($p < 0.01$). Neural activity was aligned to movement onset,
870 indicated by the black vertical line. Gray shading indicates display of the grip cue. Blue and
871 green shadings indicate mean reaction and movement times, respectively. The vertical
872 dashed line corresponds to the average time of object release. B: Cross-temporal decoding
873 of grip (left) and force (right) during the peri-movement period of the task. C: Generalization
874 index estimated as the proportion of static bins resulting from the cross-temporal decoding
875 of grip as a function of time when training and testing the classifier during preparatory and
876 executive periods of the task. D: Stable time points of the cross-temporal decoding of grip
877 (left) and force (right). Yellow squares indicate significantly stable time bins.

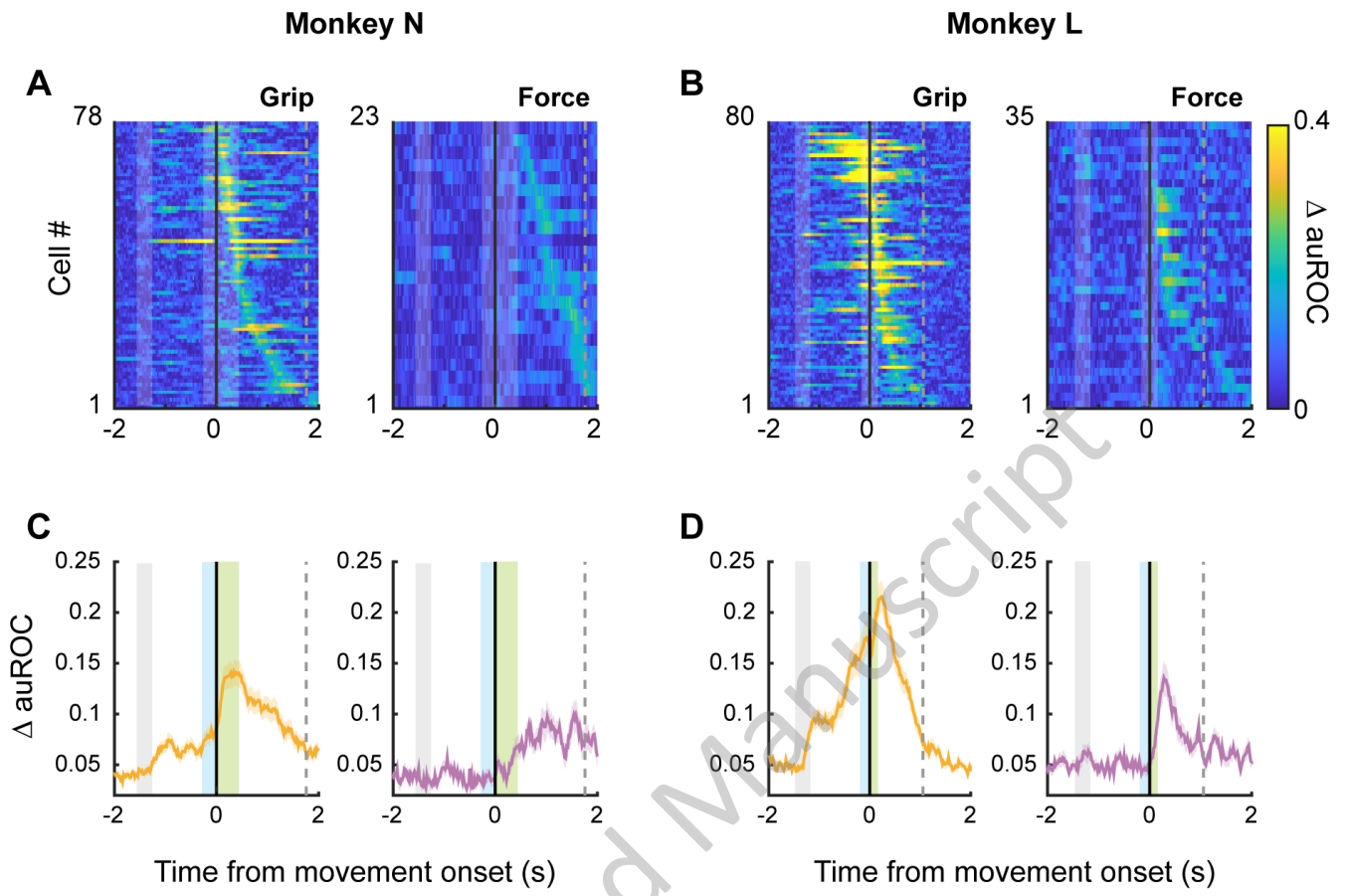
878

A

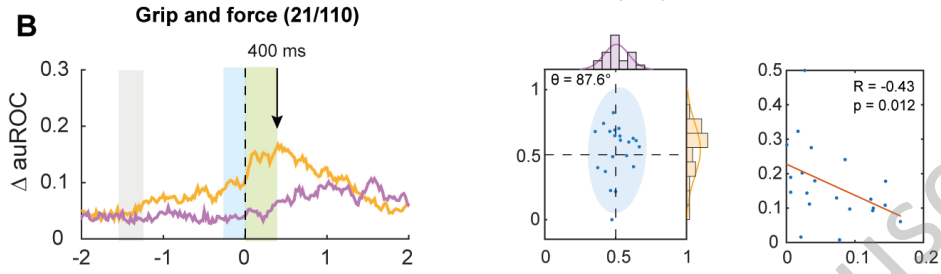
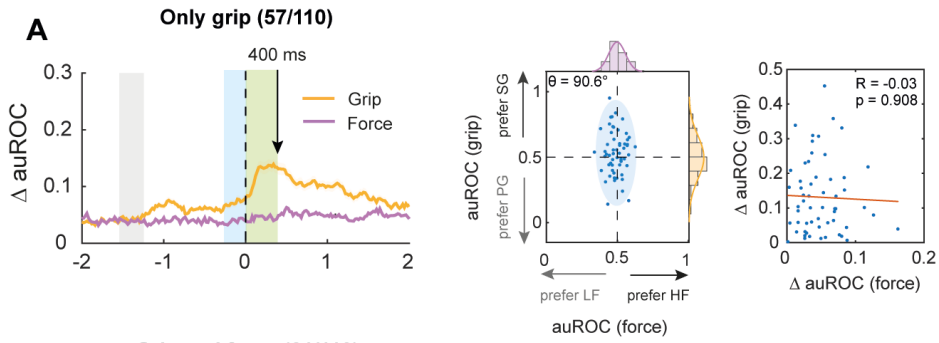
Delayed reach-to-grasp task

**B****C**

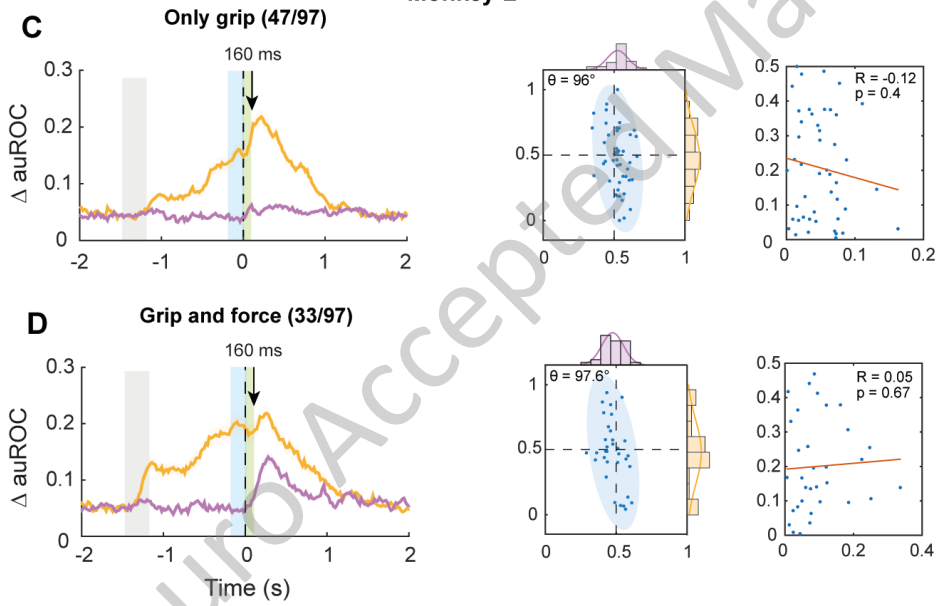


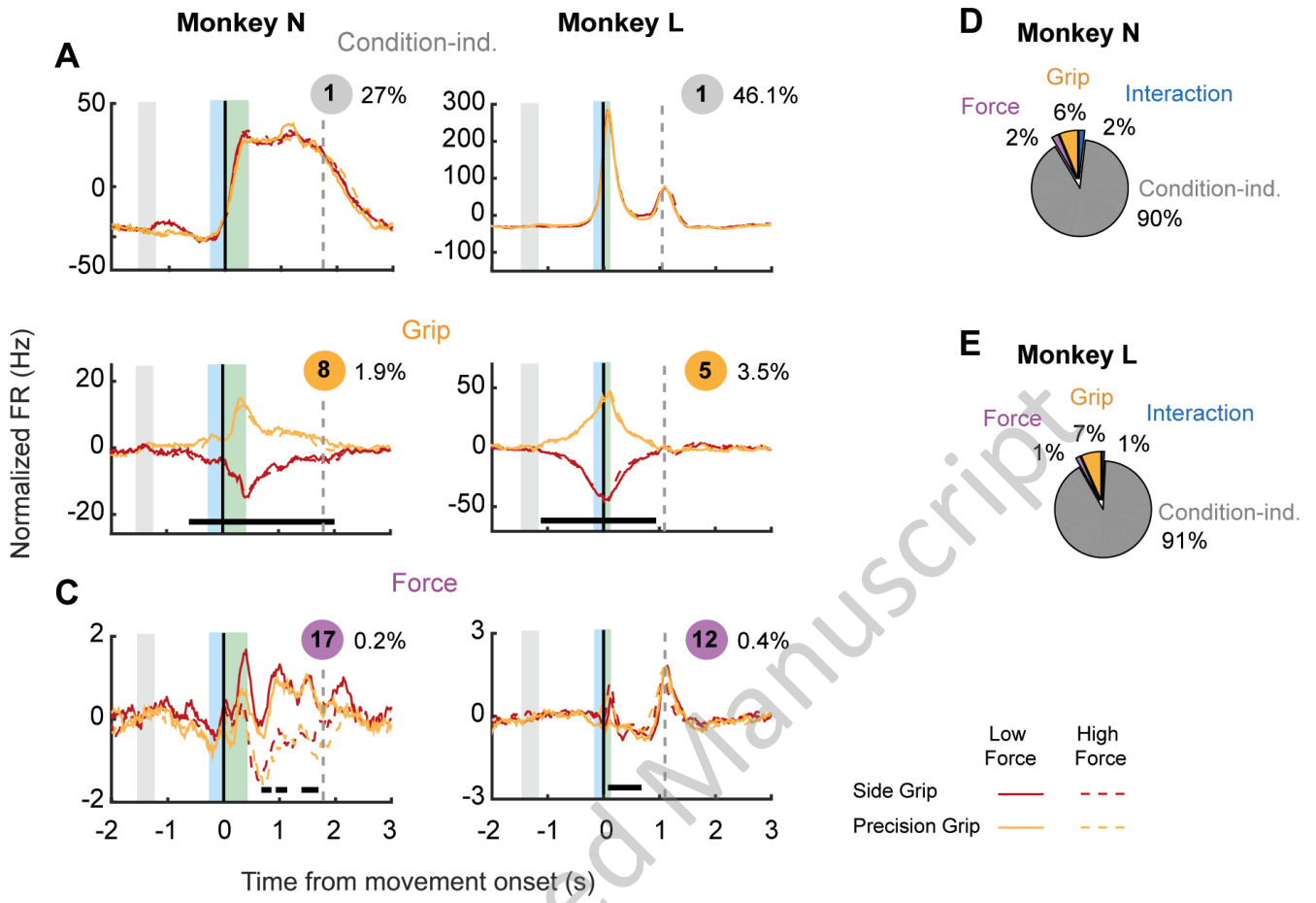


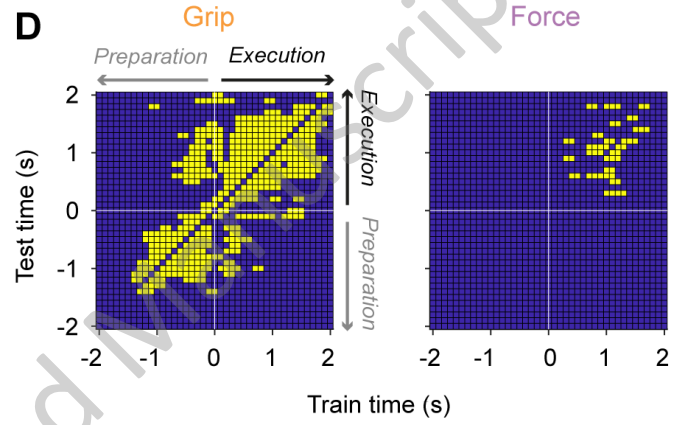
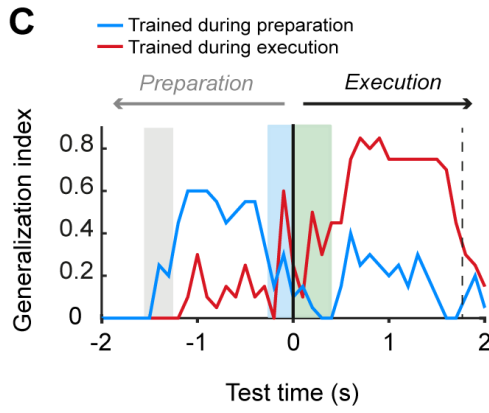
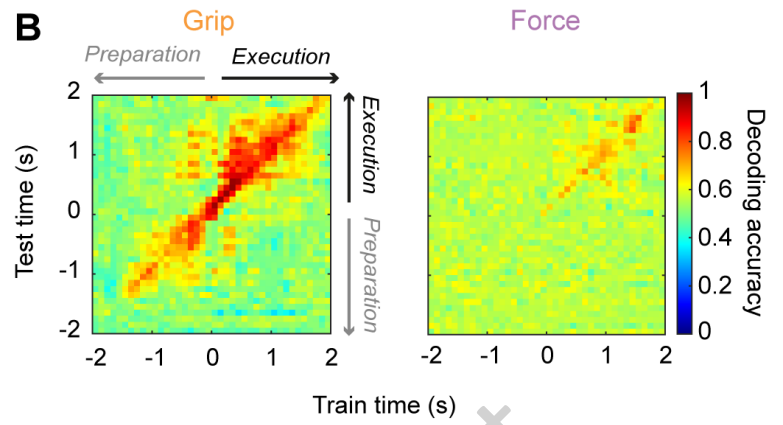
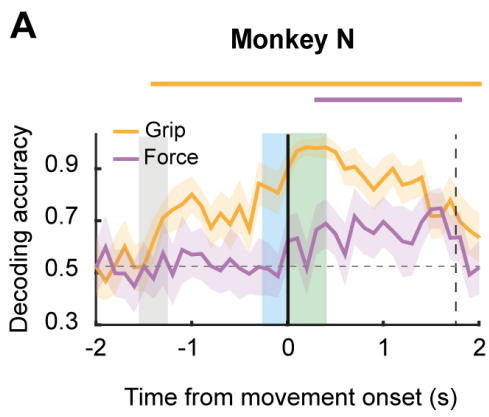
Monkey N



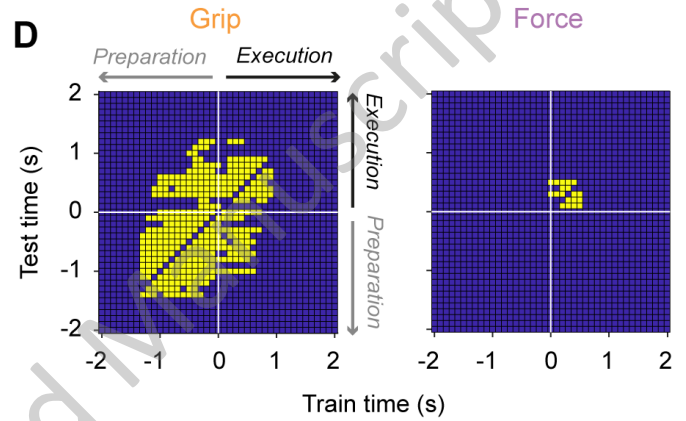
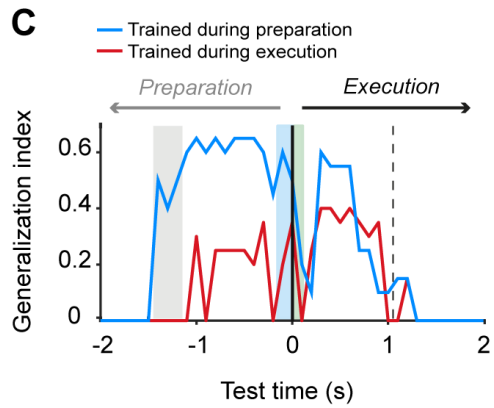
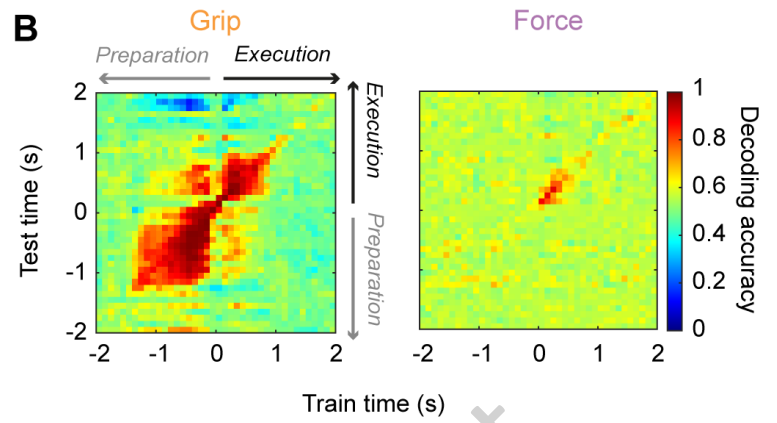
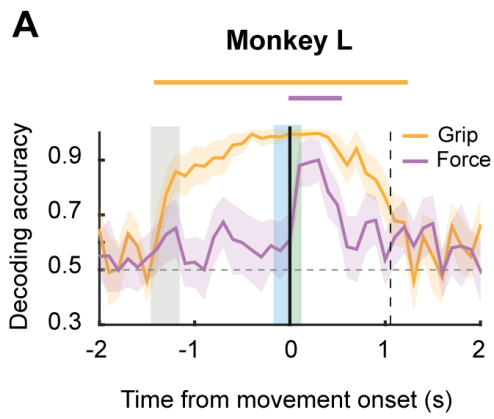
Monkey L







eNeuro Accepted Manuscript



eNeuro Accepted Manuscript